The Clinical Use of Computer-Assisted Orthopedic Surgery in Horses

Journal:	*Veterinary Surgery*
Manuscript ID	VSU-20-037.R1
Manuscript Type:	Original Article - Clinical
Keywords:	horse, orthopedic surgery, computer-assisted orthopaedic surgery, fracture repair

Abstract

Objectives: To describe clinical applications of computer-assisted orthopedic surgery (CAOS) in horses, using a navigation system coupled with a cone beam computed tomography (CBCT) unit.

Study Design: Retrospective clinical case series

Animals: Thirteen adult horses operated with CAOS.

Methods: Medical records were searched for horses that underwent CAOS between 2016 and 2019. Data retrieved included signalment, diagnosis, lameness grade prior to surgery, surgical technique and complications, anesthesia and surgery time, and information pertaining to the perioperative case management and outcome.

Results: In ten cases, surgical implants were placed in the proximal phalanx, third metatarsal bone, ulna, or medial femoral condyle, respectively. In one case, navigated trans-articular drilling was performed to promote ankylosis of the distal tarsal joints. In another case, an articular fragment of the middle phalanx was removed with the help of CAOS-guidance. In the last case, a focal osteolytic lesion of the calcaneal tuber was curetted with the aid of CAOS. In seven cases, a purpose-built frame was used for the surgical procedure. All surgeries were performed successfully and according to the preoperative plan.

Conclusion: CAOS can be an integral part of the clinical case management in equine surgery. To optimize workflow and time-efficiency, the authors recommend designating one team to operative planning and another to the execution of the surgical plan. Specialized equipment, such as the purpose-built frame, will further improve CAOS applications in equine surgery.

Clinical Significance: Once familiar with the operational principles, equine surgeons can readily apply CAOS for a broad spectrum of indications.

1 INTRODUCTION

Computer-assisted orthopedic surgery (CAOS) is well established in the human medical field.[1-4] It can improve surgical accuracy compared with intraoperative two (2D) and three dimensional (3D) imaging techniques used for surgical guidance.[5-9] In CAOS, virtual images are displayed to the surgeon to simultaneously provide real-time information on position and orientation of both the surgical anatomy and the navigated instruments. This is particularly useful in orthopedic surgery, where exact instrumentation and placement of implants are crucial, and where multiplanar orientation is often indispensable to precisely execute the surgical plan with minimally invasive approaches. In addition to the intraoperative image guidance, preoperative diagnostic image analysis and surgical planning are integral parts of CAOS.

Today, the majority of surgical navigation systems used for orthopedic surgery operate with optical tracking systems. Their function relies on tracking surgical instruments equipped with light-reflecting spheres by an infrared optical digitizer and camera array. Software, specifically designed for navigation purposes, correlates the position of the tracked surgical instruments in spatial relation to a previously gathered medical imaging dataset of the anatomical region of interest. In the context of CAOS, 3D imaging datasets with high bone definition, such as computed tomography (CT) studies, are ideally used.

In equine surgery, experimental studies have described potential applications of CAOS, specifically for the repair of distal phalanx and distal sesamoid bone fractures.[5-7, 10-11] However, specific reports of clinical applications of CAOS in horses and involving other anatomical regions are lacking. In recent years, and coupled with the steep increase of CT units in equine referral centers around the globe, the investment into CT-based CAOS technology has become a realistic avenue for equine surgical referral centers. In fact, several commercially available mobile CT-scanners can be coupled with surgical navigation systems and provide fully functional units that can be used for CAOS in large animal surgery (Fig. 1).

The aim of this study is to describe different clinical applications of CAOS in equine surgery and share first-hand experiences with this technology in a clinical setting.

2 MATERIALS AND METHODS

All orthopedic cases managed with CAOS and presented to the XXX between March 2016 and September 2019 were included. Data obtained from the medical records comprised age, sex, breed, diagnosis, lameness grade prior to surgery, surgical technique and complications, anesthesia and surgery time, and information pertaining to the perioperative case management. Whenever available, archived screen shots of the intraoperative surgical plan were reviewed and compared with postoperative CBCT scans and radiographs.

2.1 Preoperative patient preparation

Horses received benzylpenicillin sodium (30 000 IU/kg IV, Penicillin Natrium Streuli ad us. vet., Streuli Pharma AG, Uznach, Switzerland), gentamicin sulfate (6.6 mg/kg IV, Pargenta-50 ad us. vet., Dr. E. Graeub AG, Bern, Switzerland), and flunixin meglumine (1.1 mg/kg IV, Vetaflumex ad us. vet., Provet AG, Lyssach, Switzerland) approximately 1 hour prior to induction of general anesthesia. After premedication with acepromazine (0.03 mg/kg IM, Prequillan ad us. vet., Fatro S.p.A, Ozzano Emilia, Italy) 20 minutes prior to induction and sedation with romifidine (0.04 mg/kg IV, Sedivet ad us. vet., Boehringer Ingelheim, Basel, Switzerland) and levomethadone (0.05 mg/kg IV, L-Polamivet ad us. vet., MSD Animal Health GmbH, Lucerne, Switzerland), general anesthesia was induced with a combination of ketamine (2.5 mg/kg IV, Ketasol-100 ad us. vet., Dr. E. Graeub AG, Bern, Switzerland) and diazepam (0.05 mg/kg IV, Valium, Roche Pharma AG, Basel, Switzerland) and maintained with isoflurane. The anaesthetized horse was positioned on the surgery table, followed by aseptic preparation of the surgical field and draping.

A patient tracker (small patient frame, Medtronic, Louisville, CO, USA) was either percutaneously secured to the target bone using two self-tapping, threaded 3.2 mm pins (**cases 1 – 3 and 11- 13**) or attached to a purpose-built frame (**cases 4 - 10**), to which it was anchored with a spinous process clamp (open spine clamp, Medtronic) (see Fig. 2). Horses operated with the purpose-built frame had the shoe removed and the hoof cleaned and trimmed to fit in a NANRIC Ultimate shoe (NANRIC, Lawrenceburg, KY, USA) of appropriate size. Hoof shoes of different sizes were fixed with plastic screws to the purpose-built frame, in a variable dorsal-to-palmar/plantar position, so that the construct could accommodate different hoof sizes and conformations. Following aseptic preparation of the surgical site and draping of the hoof and the lower limb (up to proximal cannon bone) with sterile adhesive film (OPSITE, Smith&Nephew, London, UK), the limb was secured in the sterilized purpose-built frame using sterilized tie down straps with plastic Ladder lock buckles (see Fig. 2).

2.1.1 Preoperative imaging and planning

A mobile cone beam computed tomography (CBCT) unit (O-arm by Medtronic), was used for intra-operative 2- and 3D imaging. To complete the fully functional CT-based CAOS system the O-arm is coupled with the StealthStationS7 (Medtronic) navigation system and a carbon fiber table (Opera Swing, General Medicale Merate S.P.A., Seriate, Italy) (see Fig. 1).

Following patient preparation, a preoperative CBCT scan was acquired either in the surgical preparation area or inside the surgical theater. First, adequate positioning of the target bone in the isocenter of the gantry was confirmed with two orthogonal 2D (fluoroscopic) projections. Next, the camera of the StealthStationS7 was oriented to simultaneously detect the tracker of the O-arm gantry and the patient tracker (see Fig. 1). The 2D and 3D images were acquired remotely without exposing personnel. A standard acquisition, i.e. 192 images during one tube rotation using an exposure of 120 kV and 64 mAs, was performed. If increased spatial resolution was desired, a high-resolution scan was acquired, which doubled the acquisition time to 26 s and increased the exposure up to 128 mAs.

The acquired CBCT dataset was automatically transferred to the StealthStationS7. The surgeon and a radiologist then assessed the CT images for adequate image quality and diagnostic purposes. Whenever surgical implants were to be placed, preoperative surgical planning was performed with the S7 Cranial or S7 Spine and Trauma Software (Medtronic) (Fig. 3 A). Prior to any surgical manipulation, the O-arm was moved away from the surgical area to provide the surgeons unrestricted access to the surgical site. To initiate the navigated procedure, the surgeon made contact with the patient tracker using the navigated pointer, thus linking the subject's real anatomy with its virtual image (see Fig. 2 A).

2.1.2 Preoperative preparation of navigated instruments

For cases that required navigated drilling, a battery-powered surgical drill (Colibri II, DePuy Synthes) was mounted with a small tracker (SureTrak II clamps and tracker, Medtronic) on the instrument shaft. This was done in the immediate preoperative period while preparing the instrument table to keep surgery time as short as possible. As a final step in preparation for intraoperative guidance, the navigated instrument had to be registered and calibrated (see Fig. 2 B). To avoid re-calibration of the drill during the procedure, drill bits of different diameters had to be of the same length.

2.2 Surgical procedures

2.2.1 Screw repair using lag technique

In all cases (**1-9**) that required screw placement, CAOS served to control the drilling procedures to place 4.5 mm or 5.5 mm cortex screws in lag fashion according to the operative plan established with the help of the surgical navigation system. All horses were placed in lateral recumbency, with the exception of **case 3** (dorsal recumbency).

Anatomical fracture gap reduction of a displaced fracture was only required in **case 1**, and achieved by applying pointed bone reduction forceps under repeated 2D (fluoroscopic) imaging control.

A preoperative CBCT scan was acquired and the fracture configuration assessed in a multiplanar reconstruction of the 3D scan. Using the navigation system, a corridor for each screw was planned perpendicular to the fracture line, or centered on the lesion (for subchondral bone cysts), prior to drilling and screw placement (see Fig. 3 A). This was initiated by determining the appropriate position for the skin incision with the navigated pointer (see Fig. 2 C) followed by a stab incision reaching the surface of the target bone. Using the drill sleeve and a navigated 4.5 mm (or 5.5 mm) drill bit, the glide hole was drilled. During this step of the procedure, the surgeon closely monitored drill orientation and penetration depth on the screen of the navigation system (Fig. 4). Once the fracture plane was crossed (or the lesion entered) with the 4.5 mm (or 5.5 mm) drill bit, the drill bit and sleeve were exchanged (3.2 mm or 4.0 mm), inserted into the glide hole, and the thread hole was completed. Following countersinking, screw-length measurement, and tapping, a 4.5 mm (or 5.5 mm) cortex screw was placed in lag fashion. This was repeated until all planned screws had been introduced and sequentially had been tightened. Appropriate position and length of the implants, as well as satisfactory reduction of the fracture gaps and re-alignment of articular surfaces were assessed on a postoperative CBCT scan (see Fig. 3 B). Screws of inadequate length were replaced and the postoperative scan repeated if necessary. The tracker or purpose-built frame was removed and all skin incisions were closed with simple interrupted sutures using non-absorbable 2-0 monofilament suture material (Prolene, ETHICON, LLC., Johnson & Johnson, Zug, Switzerland).

2.2.2 Minimally invasive fragment removal

In **case 10**, CAOS guidance was used to remove a non-displaced osteochondral fragment marginal to the proximal interphalangeal joint of the left thoracic limb. Based on a preoperative CBCT scan that was acquired with the horse standing, it was assumed that the fragment originating from the dorsolateral proximal aspect of the middle phalanx would be poorly visible arthroscopically. Hence, a minimally invasive cut-down procedure was planned to remove the fragment. The horse was positioned in right lateral recumbency and the affected limb was placed in the purpose-built frame. After CBCT image acquisition, the navigated pointer was used for sporadic depth- and position-control and the fragment was removed via a 2 cm longitudinal skin incision. The skin incision was closed with simple interrupted sutures using non-absorbable 2-0 monofilament suture material (Prolene, ETHICON, LLC.).

2.2.3 Trans-articular drilling and cartilage forage

A minimally invasive trans-articular drilling procedure of the right tarsometatarsal- and distal intertarsal joints was performed in **case 11,** to induce ankylosis. The horse was positioned in right lateral recumbency with the affected leg down. After making a 3 cm longitudinal skin incision centered over the medial aspect of the right third tarsal bone, intraoperative CAOS guidance was used to precisely penetrate both the centrodistal- and the tarsometatarsal joint in a medial to lateral direction with a 3.2 mm drill bit. Thus having gained access to each joint, as much articular cartilage as possible was removed using a navigated high-speed surgical drill equipped with a telescoping 3 mm diamond-burr head (Midas Rex Legend, Medtronic). For this, the burr was passed in a fan-shaped pattern from dorsal to plantar and at increasing depth. Once cartilage removal of both articular surfaces was deemed appropriate, a CBCT scan was repeated. As forage was completed, the skin incision was closed with simple interrupted sutures using non-absorbable 2-0 monofilament suture material (Prolene, ETHICON, LLC.).

2.2.4 Plate fixation

Plating of a chronic, comminuted, transverse, articular (type 4)[12] ulnar fracture was performed in **case 12** (Fig. 5). The horse was placed in lateral recumbency with the fractured ulna uppermost. An initial CBCT scan was acquired, and the adequate plate length was determined, based on measurements made on the acquired images. A slightly curved skin incision was made over the caudal aspect of the ulna and extended 17 cm distal to the point of the olecranon. Sharp dissection was continued between the ulnaris lateralis muscle and ulnar head of the deep digital flexor tendon until the periosteum and fibrous callus of the fracture on the caudal aspect of the ulna were exposed.

A nine-hole 4.5/5.0 mm narrow Locking Compression Plate (LCP) (DePuy Synthes) was contoured and positioned over the exposed bone surface. To indicate the entry point for the first plate screw, the navigated pointer was introduced into a 3.2 mm universal drill guide sleeve and seated in the combi-hole of the LCP that was to be filled. Using the navigation system, a corridor was drawn starting from the planned entry point on the caudal cortex to the cranial cortex of the olecranon. When planning the corridors for the plate screws proximal to the anconeal process, attention was paid not to penetrate the concave medial cortex of the olecranon. Following navigated drilling and thread preparation, the first 4.5 mm cortex screw of appropriate length was placed in a neutral position, thus pressing the plate against the ulna (see Fig. 5 C).

This was repeated accordingly for each cortex screw. Whenever the desired drill-tract could be orientated perpendicular to the plane of the LCP, a 5.0 mm locking head screw (LHS) was placed. This resulted in a construct with one 5.0 mm LHS and three 4.5 mm cortex screws filling the most proximal, and two 4.5 mm cortex screws and two 5.0 mm LHS filling the most distal plate holes (Fig 5D). The central hole of the plate was directly overlying one of the fracture gaps and was therefore not filled. Following lavage with sterile isotonic fluids, the incision was closed in three layers of continuous suture patterns (PDS II 2-0 and Prolene, ETHICON, LLC., Johnson & Johnson AG, Zug, Switzerland).

2.2.5 Minimally invasive, bursoscopy-assisted, navigated bone curettage

A focal osteolytic lesion within the calcaneal tuber just distal to the insertion of the gastrocnemius tendon located in the subtendinous calcaneal bursa, was curetted with the aid of CAOS in **case 13**. The horse was placed in lateral recumbency with the affected limb uppermost. After anchoring of the tracker on the lateral aspect of the proximal third metatarsal bone, CBCT images were acquired. An endoscopic portal was made between the superficial digital flexor tendon and the long plantar ligament, 10 mm distal to the lateral retinaculum, and the subtendinous calcaneal bursa was arthroscopically inspected. An instrument portal was created proximal to the retinaculum, ipsilateral to the arthroscope. However, no cartilaginous defect of the calcaneal tuber was visualized nor accessed with an arthroscopic probe during endoscopic exploration. Using the navigated pointer, a 2 cm longitudinal skin incision was then made plantar and directly over the lytic lesion and extended through the fibrocartilaginous cap of the superficial digital flexor tendon onto the surface of the calcaneus. The necrotic bone was removed using a size 00 curette and a motorized arthroscopic burr (Synergy Arthroscopic Shaver, Arthrex AG, Belp, Switzerland). For this, trackers were mounted to both the curette and the motorized burr, using small clamps, to navigate the debridement and control penetration depth and position of the instrument heads. After copious lavage of the subtendinous calcaneal bursa, the skin incisions were closed using a simple interrupted suture pattern and non-absorbable 2-0 monofilament suture material (Prolene, ETHICON, LLC.)

2.3 Postoperative case management

All horses received one dose of benzylpenicillin sodium (30 000 IU/kg IV, Streuli Pharma AG) postoperatively. Depending on the lesion treated in each case, non-steroidal anti-inflammatory medication was continued postoperatively at the discretion of the clinician. In horses registered as companion animals, phenylbutazone (2.2 mg/kg orally twice daily, Equipalazone ad us. vet., MSD Animal Health GmbH, Lucerne, Switzerland) was usually administered, whereas horses registered as food producing animals were medicated with meloxicam (0.6 mg/kg orally once daily; Metacam, Boehringer Ingelheim, Basel, Switzerland) to provide anti-inflammation and analgesia during the postoperative period. In **cases 1, 7 and 8**, a half-limb cast was applied for 2 to 3 weeks postoperatively. In the other cases, the surgical wounds were protected either by a bandage or adhesive dressing until suture removal. Depending on the nature of the initial lesion, box rest was recommended for 3 weeks and up to 2 months. After this period of stall rest, the exercise plan for the convalescence time was individually adapted based on the findings of control examinations.

2.4 Assessment of patient preparation, imaging and surgery time, surgical complications, and outcome

For each procedure, the time for patient preparation and surgery time were determined from the anesthesia report. The time for patient preparation and imaging included positioning and aseptic surgical preparation, anchoring of the tracker or placement of the purpose-built frame, the preoperative acquisition and assessment of the CBCT images, and the surgical planning. This was defined as the anesthetic period between induction and the first skin incision, recorded in the anesthesia protocol. The surgery time was the time recorded as the time between first skin incision and the moment the horse was disconnected from the anesthesia machine.

All surgery reports were reviewed for any intraoperative complications that were recorded.

All horses were subjected to an orthopedic and radiographic control examination two months following surgery. These examinations were done either at the XXX or by the referring veterinarian. Follow-up was obtained via telephone interview with the owners at the time of manuscript preparation.

3 RESULTS

Table 1 provides a case-by-case overview of the indications and procedures included in the study.

Thirteen horses, eight mares, and five geldings with a mean age of 8.8 years (range 4-13) were included. Breed distribution was nine Warmbloods, one Standardbred, one Franches-Montagnes horse, one pony, and one Icelandic horse. The most common use of the horses was show jumping (6), followed by pleasure riding (3), dressage (1), eventing (1), racing (1), and schooling (1).

Preparation and surgery time were established for 12 of the 13 procedures. Time when surgery was started was not indicated in the protocol of **case 2**. Mean preparation time was 102 minutes (range, 55-170) and surgery time was 83 minutes (range, 30-155). The mean proportion of preparation and surgery time, in relation to the total anesthesia time, were approximately 55% and 45%, respectively.

Once the purpose-built frame was developed, it was used in all clinical cases involving target bones distal to the carpus or tarsus and for which the attending surgeon desired surgical navigation.

Intraoperative complications occurred in four cases. Inadvertent intrusion of the screw head through the cortical bone when tightening a 4.5 mm screw inserted in lag technique occurred in two cases (**6 and 9**) and a washer was applied to reach a satisfactory compression in both cases. In **case 8**, stripping of the thread occurred when tightening a 4.5 mm lag screw. The screw was removed, the glide hole was over drilled with a 5.5 mm drill, and a 5.5 mm cortex screw was subsequently placed. In **case 9**, an additional intraoperative CBCT scan had to be performed, because of inadvertent displacement of the tracker by the surgeon. This had no consequence on the outcome of the procedure due to the rapid recognition of the problem.

Postoperative scans were assessed by the operating surgeon and implant position and dimensions were found to be appropriate in all cases. In cases where the Cranial software had been used (cases 4-6, 8), the pre- and postoperative scans were merged and agreement of the actual repair with the preoperative plan was assessed by the operating surgeon. Sporadic measurement of surgical accuracy aberrations confirmed values in the range of about 1 - 2 mm, which is consistent with the findings of an experimental study.[13]

By the time clinical and radiographic recheck took place, ten horses had improved clinically (**cases 1-4, 7, 8, 10-13**). In two horses (**cases 5 and 6**) lameness remained unchanged. One horse (**case 9)** was euthanatized two weeks after surgery, and the day following hospital discharge, because of catastrophic fracture of the third metatarsal bone.

Bone healing was satisfactory in all cases that survived (12/13). **Case 9** was lost before bone healing occurred. This mare had sustained a catastrophic fracture of the third metatarsal bone, after it had returned to the farm thirteen days after the repair. The fracture had propagated to a complete, open fracture at mid-diaphysis level. The fracture plane passed through the most distal screw hole of the repair. All other screws were in situ and tightly compressed the proximal half of the third metatarsal bone. In **case 7**, excessive new bone formation, which was already present prior to surgery but to a lesser degree, was visible at the dorsal aspect of the proximal phalanx. Furthermore, a thin fracture line reaching the distal articular surface of the proximal phalanx had become apparent secondary to bone resorption. However, the clinical progression and fracture stabilization were judged appropriate.

By the time of manuscript preparation, long-term outcome (> 12 months)[14] was available for seven horses, mid-term outcome (6-12 months)[14] for three horses, and short term outcome (3-6 months)[14] for two horses. One horse had to be euthanatized (**case 9**). Nine horses had returned to their intended use. **Case 8** was sound at the walk and trot and beginning with training. Two horses (**cases 5, 6**) remained mildly lame at the trot.

4 DISCUSSION

This is the first known study to specifically report first-hand clinical experiences with CAOS in equine surgery. The introduction of CAOS to an equine referral hospital was met with skepticism and concern regarding not only its practicality but also its reliability and effectiveness. Although the information provided here does not substantiate that CAOS improves surgical accuracy and overall outcome compared to other image-guided surgical techniques, the experiences described here nonetheless assert that CBCT-based navigation and optical tracking systems can be used as an integral, practical, and reliable technology in equine orthopedic surgery. The often-debated practicality of CAOS is mainly determined by the CAOS-proficiency of the operating surgeon and CAOS-preparedness of the hospital infrastructure and personnel. With increasing experience, not only surgeons and support staff become more proficient, but they also learn to appreciate the potential advantages and pitfalls associated with CAOS. Over time, and even more so with the introduction of the purpose-built frame, CAOS has evolved to become the preferred choice for the vast majority of orthopedic surgeries at our referral practice that require multiplanar intraoperative orientation. The observation that this exposure positively influenced the case-selection, in terms of frequency of use and broadening the spectrum of indications, reflects the utility and practicality of CAOS. It also perpetrates the unanimous conviction of the authors that CAOS has produced a “better” scenario for many routine orthopedic surgeries and particularly for interventions with high demands in surgical orientation and accuracy.

Undoubtedly, the purpose-built-frame featured in this article lead the way to expanding the spectrum of CAOS applications to include "routine" orthopedic procedures involving the distal extremity and MCIII/MTIII. To create the spatial relation between the guided instruments and the target bone, a patient tracker needs to remain stably anchored in relation to the target bone. This is normally achieved by drilling pins into the target bone (see Figs. 5

B and D) that provide an angle-stable fixation for the tracker. This increases the risk of infection[15] or pin-hole fracture.[16-19] Furthermore, particularly when working on short bones of the distal extremity, interferences between the patient tracker and navigated instruments can complicate the surgery. Alternatively, the patient tracker can be secured to an external frame fixed to the extremity and maintaining a stable connection to the target bone. The presented purpose-built frame avoids these potential complications without compromising surgical accuracy[13] and stabilizes the extremity in a convenient working position.

The case material presented here included various pathologies reaching from the distal extremity to as far proximal as the elbow and stifle joint. This is only possible because of the high mobility of the O-arm unit and its gantry, which can be opened on one side to form a "C" to facilitate positioning. This allows for a time-efficient positioning of the gantry around the region of interest and rapid removal from the surgical field. During image acquisition, the gantry housing itself does not move. Furthermore, image acquisition takes less than half a minute per scan. This not only expedites the surgical workflow, but also permits all people to leave the room during image acquisition, entirely avoiding radiation exposure.

However, it needs to be considered that the O-arm was developed for computer-assisted surgery applications in humans, where cortical bone is much thinner and less dense than in horses. This was found to be a potential disadvantage for CAOS applications in horses. In **cases 7 and 9**, the extent of the fracture was underestimated based on the preoperative CBCT images. Therefore, the operating surgeons failed to detect and follow the distal end of the non-displaced fracture line to provide adequate screw compression. Underestimation of the extent of bone damage can lead to dramatic propagation of fracture lines after surgical repair.[20] The low contrast resolution within thick and dense cortical bone is due to its attenuation of low energy photons from the X-ray beam. This can be overcome by pre-hardening the X-ray beam with a filter.

In the human medical field, costs, technical complexity, and inefficiency have been major barriers for the entry of computer-assisted systems into surgical practice.[21] In order to make use of navigation systems, surgeons need to understand the operational principles, practice their application, and adapt their skill set to avoid pitfalls that may be experienced with this technology. Furthermore, no efforts must be spared to organize CAOS procedures as efficiently as possible and reduce the length of the anesthetic period. While meta-analyses of CAOS have demonstrated increased operative times compared to conventional techniques,[22] it has also been shown that operating times are strongly influenced by the learning curve of the personnel.[23] Therefore, appropriate training of the operating surgeons and technical staff, as well as the adequate distribution of tasks during the surgical preparation and procedure, need to be implemented when performing CAOS in a clinical setting.[24] Because of the heterogeneity and the low number of cases presented in this case series, as well as the number of different surgeons (four) with varying CAOS proficiency levels, the effect of the learning curve on the surgical time could not be critically assessed. In general, CAOS will lead to a shift from time spent on surgical manipulations and intraoperative orientation and imaging (45% of the entire procedure), to time spent on patient-preparation, preoperative imaging and planning (55%). The more complex the procedure is, the more drilling procedures that are made, and the more implants that are placed, the easier it is to compensate for the time invested into patient-preparation and pre- and intraoperative imaging. However, this could not be substantiated by the results because of the low number of cases and the limitations inherent to the retrospective nature of the presented study. The influence of distinct parameters on preparation and surgical times would need to be assessed in a prospective clinical trial.

A potential pitfall inherent to CAOS is the loss of surgical accuracy during the procedure. The operating surgeon needs to be aware of imminent sources for surgical accuracy aberrations, minimize the risks for these to occur, and be able to detect and correct these promptly.

Potential sources that lead to a loss in surgical accuracy include plastic deformation of the navigated instrumentation, mainly because of bending of long drill bits. In humans, this is a known phenomenon when drilling through an area of sclerotic bone.[25] In horses, the thick and dense cortical bone certainly potentiates the risk of plastic drill bit deformation. To minimize this risk, the operating surgeon should choose short drill bits whenever possible and carefully control drill bit alignment and pressures placed on the drill.

Other factors contributing to a loss of surgical accuracy have been identified for CAOS. These include instable anchoring of the tracker on a target bone of reduced density, for instance when operating on osteoporotic bone of geriatric patients[25,26] or malfunctioning of the infrared optical digitizer and camera array due to blood-contaminated reflectors.[25] In any case, surgeons must aim to promptly detect any significant loss in accuracy and assess if the virtual image accurately represents the real situation during all critical steps of the procedure. Thus, the surgeon needs to pay close attention to the tactile feedback and ensure that all actions correspond with what the virtual image is showing. In a computer-assisted drilling procedure, the surgeon not only has control over drill orientation but also over penetration-depth. Therefore, the tactile feedback of engaging or penetrating cortical bone will correspond with the position of the drill-bit tip shown on the monitor, as long as the virtual image is an accurate representation of the real situation (see Fig. 4). If discrepancies are noted, loss of surgical accuracy has to be suspected and the surgeon must critically re-assess the congruence of virtual images and reality.

In conclusion, CAOS has become an integral part of the management of routine interventions in the authors' equine referral hospital. Surgeons quickly became acquainted with the operational principles of computer-assisted surgery and soon gained confidence to use it for various orthopedic procedures, providing them with so far unmatched intraoperative orientation and control. Undoubtedly, CAOS will open new avenues to manage complex orthopedic cases reliably and successfully. Further technical innovations and equine-specific adaptions of the available instrumentation and imaging equipment are desirable to make CAOS more practical and reduce time sacrificed for patient preparation. Moreover, guidelines to optimize adequate placement of the pins and tracker for frequently encountered interventions in horses are warranted.

Acknowledgments

XXX

Conflicts of interest

The authors declare no conflict of interest related to this report.

References

1. Schouten R, Lee R, Boyd M, et al. Intra-operative cone-beam CT (O-arm) and stereotactic navigation in acute spinal trauma surgery. *J Clin Neurosci.* 2012;19(8):1137-1143.
2. Van de Kelft E, Costa F, Van der Planken D, Schils F. A prospective multicenter registry on the accuracy of pedicle screw placement in the thoracic, lumbar, and sacral levels with the use of the O-arm imaging system and StealthStation Navigation. *Spine* Philadelphia, PA, USA. 2012;37(25):E1580-1587.
3. Lee DJ, Kim SB, Rosenthal P, Panchal RR, Kim KD. Stereotactic guidance for navigated percutaneous sacroiliac joint fusion. *J Biomed Res.* 2016;30(2):162-167.
4. Frizon LA, Shao J, Maldonado-Naranjo AL, et al. The Safety and Efficacy of Using the O-Arm Intraoperative Imaging System for Deep Brain Stimulation Lead Implantation. *Neuromodulation.* 2018;21(6):588-592.
5. Gygax D, Lischer C, Auer JA. Computer-assisted surgery for screw insertion into the distal sesamoid bone in horses: an in vitro study. *Vet Surg.* 2006;35(7):626-633.
6. Andritzky J, Rossol M, Lischer C, Auer JA. Comparison of computer-assisted surgery with conventional technique for the treatment of axial distal phalanx fractures in horses: an in vitro study. *Vet Surg.* 2005;34(2):120-127.
7. Rossol M, Gygax D, Andritzky-Waas J, et al. Comparison of computer assisted surgery with conventional technique for treatment of abaxial distal phalanx fractures in horses: an in vitro study. *Vet Surg.* 2008;37(1):32-42.
8. Tian NF, Huang QS, Zhou P, et al. Pedicle screw insertion accuracy with different assisted methods: a systematic review and meta-analysis of comparative studies. *Eur Spine J.* 2011;20(6):846-859.

9. Cheng T, Zhao S, Peng X, Zhang X. Does computer-assisted surgery improve postoperative leg alignment and implant positioning following total knee arthroplasty? A meta-analysis of randomized controlled trials? *Knee Surg Sports Traumatol Arthrosc.* 2012; 20(7):1307-1322.

10. Schwarz CS, Rudolph T, Koval JH, Auer JA. Comparison of the VetGate and SurgiGATE 1.0 Computer Assisted Surgery Systems for Insertion of Cortex Screws across the Distal Phalanx in Horses: An In Vitro Study. *Pferdeheilkunde* 2017; 33; 120-132.

11. Schwarz CS, Rudolph T, Koval JH, Auer JA. Introduction of 3.5 mm and 4.5 mm Cortex Screws into the Equine Distal Sesamoid Bone with Help of the VetGate Computer Assisted Surgery Systems and Comparison of the Results with those Achieved with the SurgiGATE 1.0 System: An In Vitro Study. *Pferdeheilkunde* 2017; 33; 223-230.

12. Donecker JM, Bramlage LR, Gabel AA. Retrospective analysis of 29 fractures of the olecranon process of the equine ulna. *J Am Vet Med Assoc.* 1984;185(2):183-189.

13. XXX. Assessment of surgical accuracy for computer-assisted orthopedic surgery of equine extremities facilitated by the use of a purpose-built frame. Submitted to *Vet Surg*. 2020.

14. Cook JL, Evans R, Conzemius MG, et al. Proposed definitions and criteria for reporting time frame, outcome, and complications for clinical orthopedic studies in veterinary medicine. *Vet Surg.* 2010;39(8):905-908.

15. Sikorski JM, Blythe MC. Learning the vagaries of computer-assisted total knee replacement. *J Bone Joint Surg Br.* 2005;87(7):903-910.

16. Bonutti P, Dethmers D, Stiehl JB. Case report: femoral shaft fracture resulting from femoral tracker placement in navigated TKA. *Clin Orthop Relat Res.* 2008;466(6):1499-1502.

17. Li CH, Chen TH, Su YP, Shao PC, Lee KS, Chen WM. Periprosthetic femoral supracondylar fracture after total knee arthroplasty with navigation system. *J Arthroplasty.* 2008;23(2):304-307.

18. Hoke D, Jafari SM, Orozco F, Ong A. Tibial shaft stress fractures resulting from placement of navigation tracker pins. *J Arthroplasty.* 2011;26(3):504.e505-508.

19. Jung KA, Lee SC, Ahn NK, Song MB, Nam CH, Shon OJ. Delayed femoral fracture through a tracker pin site after navigated total knee arthroplasty. *J Arthroplasty.* 2011;26(3):505.e509-505.e511.

20. Genton M, Vila T, Olive J, Rossignol F. Standing MRI for surgical planning of equine fracture repair. *Vet Surg.* 2019;48(8):1372-1381.

21. Stiehl JB. Computer-Assisted Surgery: Pros and Cons. *In: Scuderi G., Tria A., eds. Minimally Invasive Surgery in Orthopedics.* Cham, Switzerland: Springer; 2016:1-9.

22. Bauwens K, Matthes G, Wich M, et al. Navigated total knee replacement. A meta-analysis. *J Bone Joint Surg Am.* 2007;89(2):261-269.

23. Thorey F, Klages P, Lerch M, Florkemeier T, Windhagen H, von Lewinski G. Cup positioning in primary total hip arthroplasty using an imageless navigation device: is there a learning curve? *Orthopedics.* 2009;32(10 Suppl):14-17.

24. Windhagen H, Thorey F, Ostermeier S, Emmerich J, Wirth CJ, Stukenborg-Colsman C. Das Navigatorkonzept. *Der Orthopäde.* 2005;34(11):1125-1130.

25. Bae DK, Song SJ. Computer assisted navigation in knee arthroplasty. *Clin Orthop Surg.* 2011;3(4):259-267.

26. Stockl B, Nogler M, Rosiek R, Fischer M, Krismer M, Kessler O. Navigation improves accuracy of rotational alignment in total knee arthroplasty. *Clin Orthop Relat Res.* 2004(426):180-186.

Figure legends

Figure 1: Overview of a computer-assisted surgery within the surgical theater after preoperative image acquisition, displaying the necessary equipment for imaging, planning and navigation, i.e. the O-arm imaging unit coupled with the StealthStation navigation system (both Medtronic). Please note that the beacon of the camera is oriented to simultaneously detect both patient- and gantry-tracker. Two teams are present in the room, one designated to imaging and planning and the other to the navigated surgery. The door to the surgery suite has been opened to roll out the imaging unit and give way to the surgical team.

Figure 2: Key elements of a computer-assisted orthopedic procedure are shown: Following image acquisition, the surgeon contacts the patient tracker with the navigated pointer. This initiating step of any computer-assisted procedure with an optical tracking system is commonly referred to as "patient registration" (A). It is necessary to link the virtual data set with the real surgical anatomy. In this particular case, the patient tracker is anchored to the purpose-built frame. Instrument calibration (B) includes a sequence of four consecutive steps to identify the plane, tip, and long-axis of the instrument. Here, the navigated pointer indicates the long-axis of a surgical drill. Identification of anatomical landmarks: Whenever possible, the surgeon should critically assess the accuracy of the registration by contacting palpable anatomical landmarks with the navigated pointer (C) and ensure agreement with the virtual data set. Here, the appropriate site for the skin incision is determined with the navigated pointer. Finally, a navigated drilling procedure (D) is shown from a perspective opposite to the localizer camera.

Figure 3: Screen shots of the Cranial Software (Medtronic) displaying (A) the preoperative plan for the repair of a complete bi-articular proximal phalanx fracture (**case 8**). Each colored line represents the planned core axis of a screw implant. (B) Merged pre- and postoperative cone beam computed tomography scans including the placed implants. The fracture is well

reduced despite the most dorsoproximal screw being positioned slightly off plan (blue line). Also, note the beam-hardening artefact caused by the metallic implants and the strap and buckle of the purpose-built frame in the volumetric reconstruction, bottom right. (C) Pre- and (D) postoperative dorsopalmar radiographs.

Figure 4: Intraoperative photograph of a computer-assisted repair of a short incomplete sagittal fracture of the proximal phalanx (**case 6**). The surgeons are closely controlling drill orientation and penetration depth on the monitor. Moreover, it is of critical importance that the surgeon pays attention to the tactile feedback of engaging or penetrating cortical bone, which has to correspond with the position of the drill-bit tip shown on the monitor.

Figure 5: Plate fixation of a chronic, comminuted articular ulna fracture (**case 12**): (A) Preoperative mediolateral radiograph. (B) Photograph of the preoperative image acquisition. Note that the large-bore gantry of the O-arm is slightly tilted to ensure that the entire olecranon process lies within the imaging isocenter, and the position of the patient tracker (arrow) on the antebrachium. (C) Intraoperative photograph of the surgeon monitor at the beginning of the drilling procedure. Note the green corridor planned for the first screw. The surgeon is still adapting the orientation of the drill, as the projection of the drill bit (yellow cylinder) is not yet overlapping with the preoperative plan. (D) Mediolateral radiograph taken three months postoperatively. One of the pin-holes for anchoring the patient tracker is still visible in the diaphysis of the radius (arrow head).

Table

Table 1: Overview of all cases operated by means of computer-assisted orthopedic surgery.

<table>
<tr><th>Case</th><th>Diagnosis</th><th>Surgical procedure</th><th>Position of tracker</th><th>Preparation time (min)</th><th>Surgery time (min)</th></tr>
<tr><td>1</td><td>P1 palmar eminence fracture</td><td rowspan="9">Screw repair using lag technique</td><td>Dorsal, mid-diaphyseal P1</td><td>55</td><td>125</td></tr>
<tr><td>2</td><td>Central tarsal bone fracture</td><td>Proximolateral aspect of MT III</td><td>Not recorded</td><td>Not recorded</td></tr>
<tr><td>3</td><td>Subchondral bone cyst in medial femoral condyle</td><td>Lateral femoral trochlear ridge</td><td>74</td><td>85</td></tr>
<tr><td>4</td><td rowspan="3">Short incomplete sagittal fracture of P1</td><td rowspan="7">Purpose-built frame</td><td>70</td><td>35</td></tr>
<tr><td>5</td><td>75</td><td>30</td></tr>
<tr><td>6</td><td>86</td><td>60</td></tr>
<tr><td>7</td><td rowspan="2">Complete bi-articular fracture of P1</td><td>170</td><td>75</td></tr>
<tr><td>8</td><td>110</td><td>95</td></tr>
<tr><td>9</td><td>Incomplete frontal articular fracture of proximal MT III</td><td>105</td><td>135</td></tr>
<tr><td>10</td><td>P2 proximal, articular border-fragment</td><td>Fragment removal</td><td>105</td><td>45</td></tr>
<tr><td>11</td><td>Osteoarthritis of the distal tarsal joints</td><td>Trans-articular drilling and cartilage forage</td><td>Proximomedial aspect of MT III</td><td>150</td><td>70</td></tr>
<tr><td>12</td><td>Type 4 ulnar fracture</td><td>Plate fixation</td><td>Proximolateral aspect of radius</td><td>105</td><td>155</td></tr>
<tr><td>13</td><td>Focal lytic lesion within the calcaneus and into the intertendinous calcaneal bursa, superimposed by the fibrocartilagenous cap of the SDFT</td><td>Bone curettage</td><td>Proximolateral aspect of MT III</td><td>125</td><td>90</td></tr>
</table>

Abbreviations: MT III: third metatarsal bone; P1: proximal phalanx; P2: middle phalanx; SDFT: superficial digital flexor tendon.

Figure 1: Overview of a computer-assisted surgery within the surgical theater after preoperative image acquisition, displaying the necessary equipment for imaging, planning and navigation, i.e. the O-arm imaging unit coupled with the StealthStation navigation system (both Medtronic). Please note that the beacon of the camera is oriented to simultaneously detect both patient- and gantry-tracker. Two teams are present in the room, one designated to imaging and planning and the other to the navigated surgery. The door to the surgery suite has been opened to roll out the imaging unit and give way to the surgical team.

252x167mm (300 x 300 DPI)

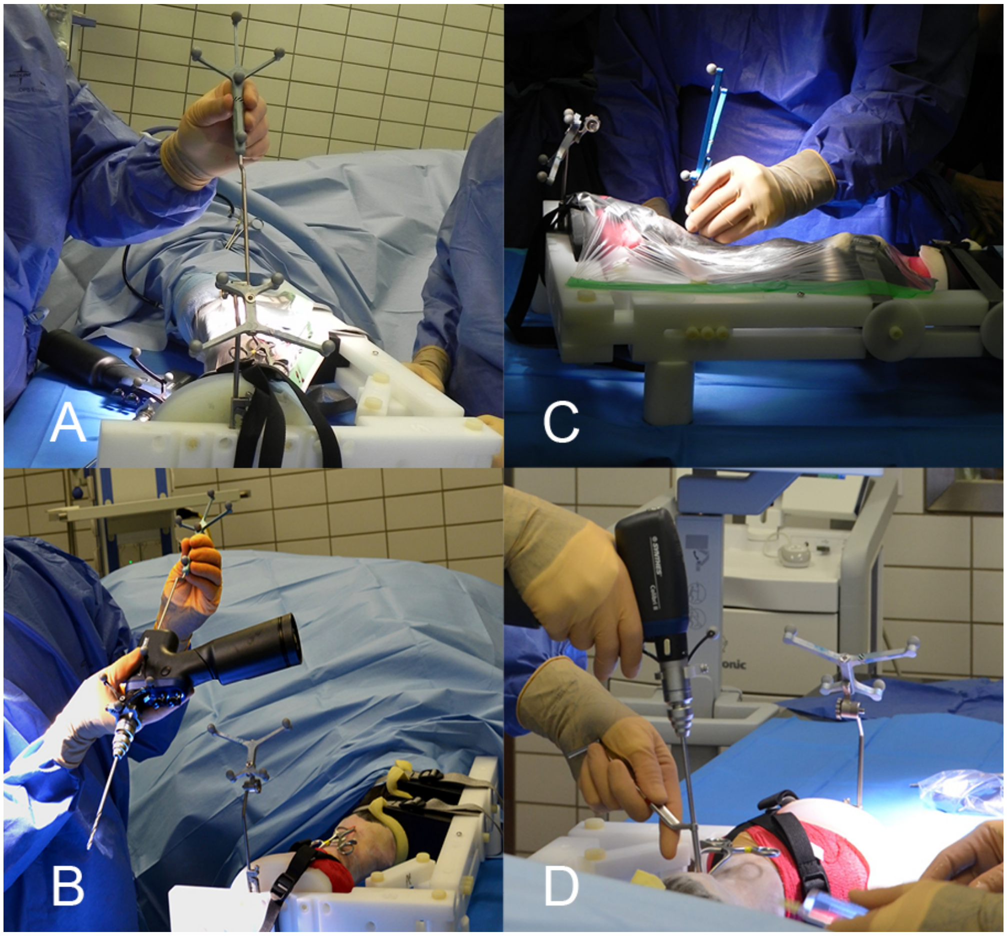

Figure 2: Key elements of a computer-assisted orthopedic procedure are shown: Following image acquisition, the surgeon contacts the patient tracker with the navigated pointer. This initiating step of any computer-assisted procedure with an optical tracking system is commonly referred to as "patient registration" (A). It is necessary to link the virtual data set with the real surgical anatomy. In this particular case, the patient tracker is anchored to the purpose-built frame. Instrument calibration (B) includes a sequence of four consecutive steps to identify the plane, tip, and long-axis of the instrument. Here, the navigated pointer indicates the long-axis of a surgical drill. Identification of anatomical landmarks: Whenever possible, the surgeon should critically assess the accuracy of the registration by contacting palpable anatomical landmarks with the navigated pointer (C) and ensure agreement with the virtual data set. Here, the appropriate site for the skin incision is determined with the navigated pointer. Finally, a navigated drilling procedure (D) is shown from a perspective opposite to the localizer camera.

319x297mm (72 x 72 DPI)

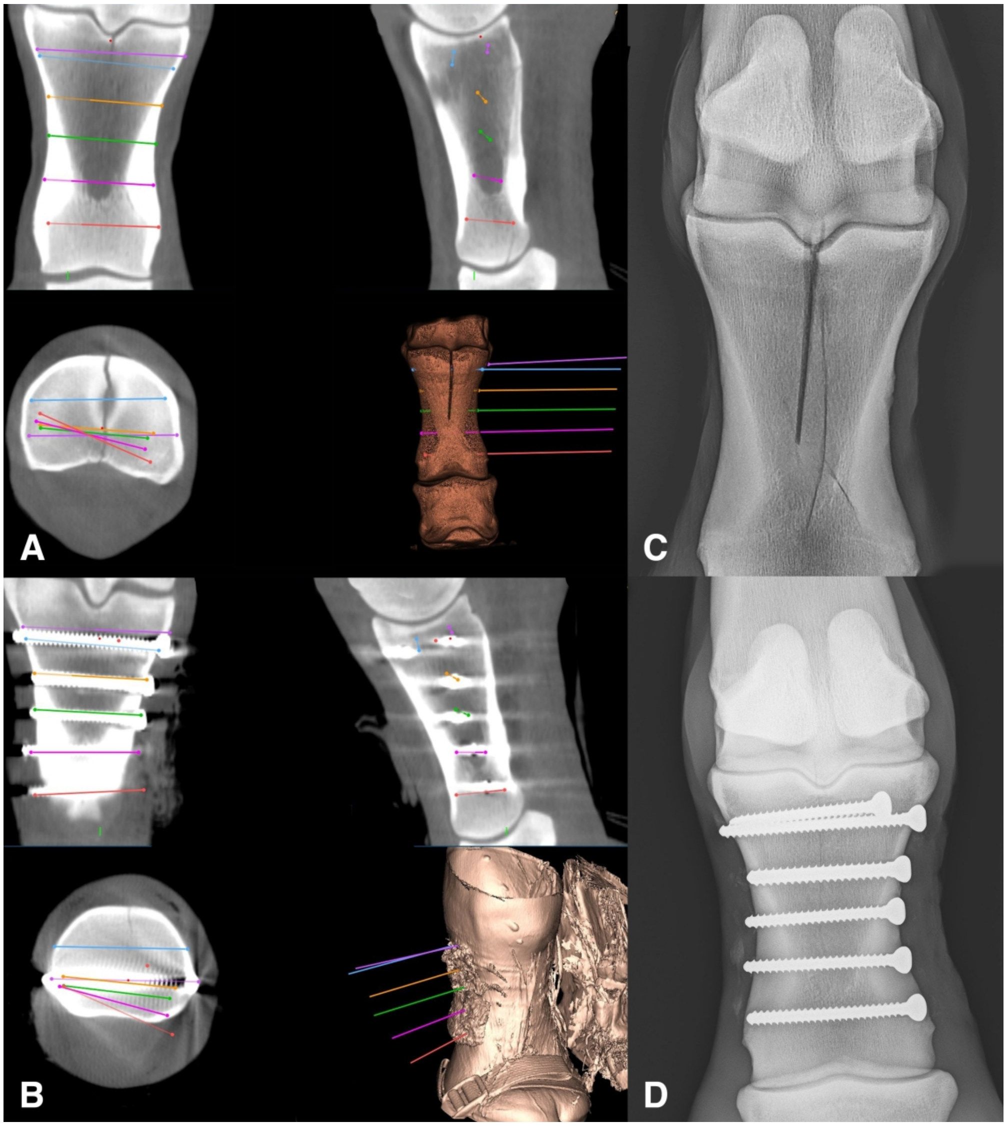

Figure 3: Screen shots of the Cranial Software (Medtronic) displaying (A) the preoperative plan for the repair of a complete bi-articular proximal phalanx fracture (case 8). Each colored line represents the planned core axis of a screw implant. (B) Merged pre- and postoperative cone beam computed tomography scans including the placed implants. The fracture is well reduced despite the most dorsoproximal screw being positioned slightly off plan (blue line). Also, note the beam-hardening artefact caused by the metallic implants and the strap and buckle of the purpose-built frame in the volumetric reconstruction, bottom right. (C) Pre- and (D) postoperative dorsopalmar radiographs.

296x331mm (300 x 300 DPI)

Figure 4: Intraoperative photograph of a computer-assisted repair of a short incomplete sagittal fracture of the proximal phalanx (case 6). The surgeons are closely controlling drill orientation and penetration depth on the monitor. Moreover, it is of critical importance that the surgeon pays attention to the tactile feedback of engaging or penetrating cortical bone, which has to correspond with the position of the drill-bit tip shown on the monitor.

417x276mm (300 x 300 DPI)

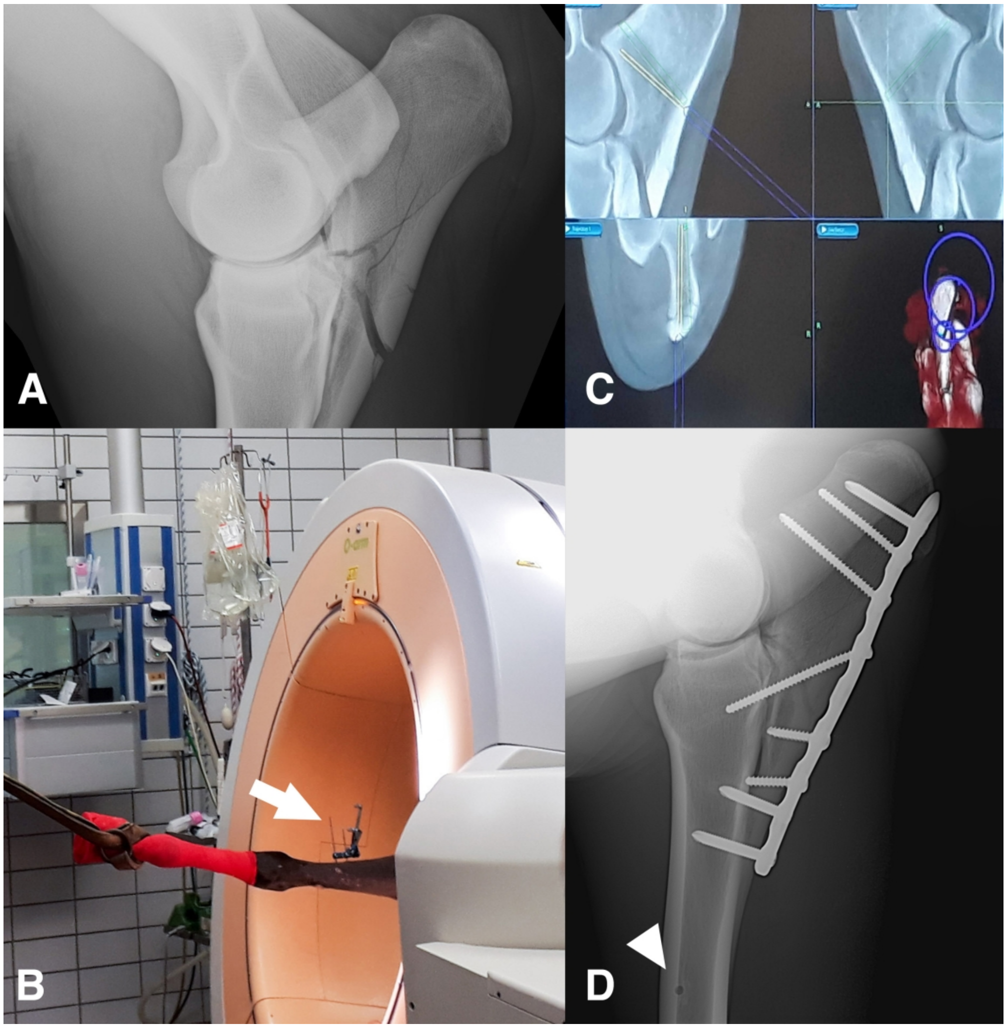

Figure 5: Plate fixation of a chronic, comminuted articular ulna fracture (case 12): (A) Preoperative mediolateral radiograph. (B) Photograph of the preoperative image acquisition. Note that the large-bore gantry of the O-arm is slightly tilted to ensure that the entire olecranon process lies within the imaging isocenter, and the position of the patient tracker (arrow) on the antebrachium. (C) Intraoperative photograph of the surgeon monitor at the beginning of the drilling procedure. Note the green corridor planned for the first screw. The surgeon is still adapting the orientation of the drill, as the projection of the drill bit (yellow cylinder) is not yet overlapping with the preoperative plan. (D) Mediolateral radiograph taken three months postoperatively. One of the pin-holes for anchoring the patient tracker is still visible in the diaphysis of the radius (arrow head).

248x253mm (300 x 300 DPI)